Korean J. Chem. Eng., 33(1), 46-56 (2016)
DOI: 10.1007/s11814-015-0100-4

pISSN: 0256-1115
eISSN: 1975-7220

Optimization study of pressure-swing distillation for the separation process of a maximum-boiling azeotropic system of water-ethylenediamine

Alyssa Marie Fulgueras*, Jeeban Poudel, Dong Sun Kim*, and Jungho Cho*,†**

*Department of Chemical Engineering, Kongju National University,
275 Budae-dong, Cheonan-si, Seobuk-gu, Chungcheongnam-do 331-717, Korea
**Department of Mechanical Engineering, Kongju National University,
275 Budae-dong, Cheonan-si, Seobuk-gu, Chungcheongnam-do 331-717, Korea
(*Received 12 March 2015 • accepted 12 May 2015*)

Abstract−The separation of ethylenediamine (EDA) from aqueous solution is a challenging problem because its mixture forms an azeotrope. Pressure-swing distillation (PSD) as a method of separating azeotropic mixture were investingated. For a maximum-boiling azeotropic system, pressure change does not greatly affect the azeotropic composition of the system. However, the feasibility of using PSD was still analyzed through process simulation. Experimental vapor-liquid equilibrium data of water-EDA system was studied to predict the suitability of thermodynamic model to be applied. This study performed an optimization of design parameters for each distillation column. Different combinations of operating pressures for the low- and high-pressure columns were used for each PSD simulation case. After the most efficient operating pressures were identified, two column configurations, low-high (LP+HP) and high-low (HP+LP) pressure column configuration, were further compared. Heat integration was applied to PSD system to reduce low and high temperature utility consumption.

Keywords: Pressure-swing Distillation, Vapor-liquid Equilibrium (VLE), Water-ethylenediamine, Maximum-boiling Azeotrope, Process Simulation

INTRODUCTION

Ethylenediamine (ethane-1,2-diamine), also known as EDA (edamine), is widely used in large quantities in the chemical industry, such as in the manufacture of fuel additives, bleach activators, chelating agents, and corrosion inhibitors [1]. EDA is a colorless, thick, water-soluble liquid with an ammonia odor. It is extremely hygroscopic and freely soluble in water, forming a hydrate. Thus, water is a common impurity in EDA, aside from the presence of other impurities in the commercial product, which is determined by the method of preparation employed [2,3]. However, the recovery of pure EDA from an aqueous EDA solution is a challenging problem since the water-EDA mixture forms an azeotrope at about 118.5 °C [2,4]. Moreover, the normal boiling point of EDA at approximately 117 °C is close to that of water, which makes the separation of its binary mixture difficult using conventional distillation method. EDA can be purified from water by using a special distillation method.

Based on an earlier study by Lichtenwalter [4], a method was discovered where the formerly difficult separation of EDA and water might be effectively accomplished with a high recovery of EDA by subjecting the aqueous EDA mixture to distillation in the presence of a high-boiling extraction solvent or agent for EDA. The water is distilled off overhead, and the bottoms mixture consisting of EDA and solvent is resolved in a second simple distillation wherein EDA is recovered at the top [4]. A similar study on this separation method was analyzed by Shen [5], which focuses on the extractive distillation feasibility studies with a light entrainer to separate maximum-boiling azeotropic mixtures.

Based on the literature, PSD is often mentioned as an alternative method to generally applied azeotropic or extractive distillation that eliminates the use of a separating agent for the separation of binary azeotropes [6]. PSD method is only applicable for azeotropes whose composition can be shifted substantially by changing the system pressure. Pressure changes can have a great effect on the vapor-liquid equilibrium compositions of azeotropic mixtures, which could indicate the possibility of using PSD as a method of separating azeotropes [7]. For PSD to be practical, the azeotropic composition must vary at least 5 percent, over a moderate pressure range (not more than 10 atmospheres between the two pressures). With a very large pressure range, refrigeration may be required for condensation of the low-pressure distillate or an impractically high reboiler temperature may result in the high-pressure column [8].

Water-EDA mixture forms a maximum-boiling azeotrope, but the investigation of the design for a maximum-boiling azeotropic system is very limited since the majority of the literature published has focused on the separation of minimum-boiling azeotropes [6]. For a maximum-boiling distillation, research studies [9,10] showed that the effect of pressure on the azeotrope is small; thus, it is expected that PSD method might not be economically attractive. However, that would be the case for minimum-boiling azeotropes since the circulating streams are distillates that must be vaporized and condensed, thus having the tendency of high energy consumption,

†To whom correspondence should be addressed.
E-mail: jhcho@kongju.ac.kr

large heat exchangers, and higher number of column trays. On the contrary, in the case of a maximum-boiling azeotrope, the circulating streams are the bottoms, so the recycle streams are liquids that do not need to be vaporized [9]. Therefore, PSD system may still be applicable despite having relatively small changes in the azeotropic composition with pressure.

According to research studies [11,12] on the separation of water-EDA mixture, PSD can also be applied in which columns are operated at different pressure range. In the study by Gabor et al. and Kopasz et al. [13,14], pressures are operated at 0.1 and 8 bar with a difference of about 26 mol% between the two azeotropic compositions. Based on another study by Kopasz et al. [15], the column pressures are operated at 1.01 and 8 bar with a 17 mol% difference between the azeotropic compositions. Nonetheless, even though water-EDA mixture can form a maximum-boiling azeotrope at atmospheric pressure, this azeotrope completely breaks at about 4-4.5 bar [16,17]. At high pressure, separation can be performed using a single distillation column with a high number of trays due to the low relative volatility at low water concentrations. But, using a high number of trays is not economically appealing in the industry. Therefore, PSD as a method of separating water-EDA mixture using different sets of pressure were investigated. The main purpose of this study was to analyze and optimize the separation method through PSD using process simulation. Based on published journals [18-20], modeling and optimization of distillation columns were analyzed using process simulators such as PRO/II, Aspen Plus and ChemCAD. The column specifications such as the number of theoretical stages, reflux ratio and feed stage locations were the objectives of optimization study. The effect of column configuration and heat integration on the overall energy consumption of the optimized PSD system were also compared.

VAPOR-LIQUID EQUILIBRIUM ANALYSIS

For the process simulation and modeling study, the analysis of the vapor-liquid equilibrium (VLE) of the system involved is very important. Based on studies about water-EDA system [11-15], the VLE plot forms a maximum-boiling azeotrope at different pressures. At low pressure of 0.1 bar, the azeotropic composition of the system is 47 mol% water with an azeotropic temperature of 62.2 °C. At atmospheric pressure of 1.01 bar, the azeotropic composition shifts to 39 mol% water with a corresponding azeotropic temperature of 120.6 °C. At high pressure of 8 bar, the azeotropic composition and temperature shifts to 21 mol% water and 199.5 °C. On the contrary, based on literature [16,17], the water-EDA azeotrope breaks at 4.0 bar and completely breaks at 4.5 bar. In this study, PRO/II with PROVISION v9.2 was used to model and optimize the PSD process for the separation of water-EDA mixture. The built-in VLE data in PRO/II was analyzed as well. The VLE diagram at different

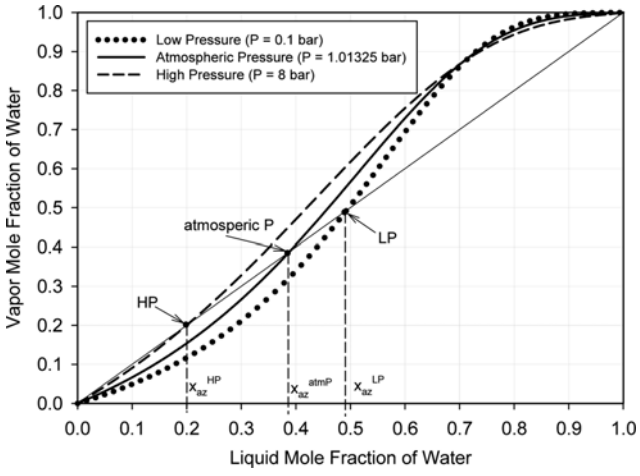

Fig. 1. x-y Diagram at different pressures based on PRO/II built-in VLE data for water-EDA.

Table 1. Built-in NRTL BIPs of water-EDA system in PRO/II

Built-in NRTL BIPs	
Parameter	Value
B_{12}	1118.6
B_{21}	−558.73
α_{12}	0.79070

Table 2. References of experimental VLE data at different pressures

Expt. data set #	Pressure (mmHg)		DDB set no.	No. of points	Reference	Volume and page
1	Low pressure	100.0	1974	26	RIVENQ F., BULL.SOC.CHIM.FR., 1606 (1963).	Vol.I Part.1, Page 211
2		200.0	1973	25		Vol.I Part.1, Page 212
3		400.0	1972	26		Vol.I Part.1, Page 213
4		600.0	1971	25		Vol.I Part.1, Page 214
5	Atmospheric pressure	760.0	1597	20	SCHMELZER J., QUITZSCH K., Z.PHYS.CHEM. (LEIPZIG), 252,280 (1973).	Vol.I Part.1, Page 218
6	High pressure	1345.2	1654	14	HIRATA M., SUDA S., HAKUTA T., NAGAHAMA K., J.CHEM.ENG.JPN., 2,143 (1969).	Vol.I Part.1, Page 206
7		2044.4	1655	13		Vol.I Part.1, Page 207
8		2774.0	1656	10		Vol.I Part.1a, Page 178
9		3480.8	1657	9		Vol.I Part.1, Page 208
10		4195.2	1658	10		Vol.I Part.1, Page 209
11		4909.6	1659	10		Vol.I Part.1, Page 210

pressures based on the PRO/II built-in data is illustrated in Fig. 1.

The VLE plot in Fig. 1 was calculated based on non-random two-liquid (NRTL) model. For most binary systems that involve liquid activity, the NRTL model is commonly applied, especially to partially miscible and completely miscible systems. For strongly nonideal mixtures, the NRTL equation often provides a good representation of experimental data if care is exercised in the data reduction to obtain the adjustable parameters [21-23]. The built-in NRTL binary interaction parameters (BIP) in PRO/II are listed in Table 1.

Experimental VLE data of water-EDA system at different pressures were also analyzed. The experimental data were obtained from DECHEMA Chemistry Data or Dortmund Data Bank (DDB). Table 2 lists the references of experimental VLE data at different pressures. Using NRTL model with the built-in BIPs in PRO/II, the VLE plot was drawn and fitted with each experimental VLE data from literature. The built-in azeotropic data of the system and boiling points of the pure components at different pressure are summarized in Table 3. However, the built-in NRTL plot shows an apparent deviation with the experimental data. Thus, thermodynamic data regression must be performed to minimize the deviations of the experimental VLE data with the equilibrium plot calculated based on NRTL model using the built-in BIPs in PRO/II. Using Thermo Data Manager (TDM) in PRO/II, data regression can be performed. The regression equation based on NRTL model for a 3-parameter equation is shown in Eqs. (1) and (2) and the objective function (ObjFcn) equation based on relative error is shown in Eq. (3) where $K_{exp,ij}$ and $K_{calc,ij}$ denote the experimental and calculated K-value of component i and j, respectively.

$$\ln\gamma_i = \frac{\Sigma_j \tau_{ji} G_{ji} x_j}{\Sigma_k G_{ki} x_k} + \sum_j \frac{G_{ji} x_j}{\Sigma_k G_{kj} x_k}\left(\tau_{ij} - \frac{\Sigma_k x_k \tau_{kj} G_{kj}}{\Sigma_k G_{kj} x_k}\right) \quad (1)$$

$$\tau_{ji} = a_{ij} + \frac{b_{ij}}{T} + \frac{c_{ij}}{T^2} \quad (2)$$

$$\mathbf{ObjFcn} = \sum_{i=obs}\sum_{j=vars} w_i\left[\frac{K_{exp,ij} - K_{calc,ij}}{K_{exp,ij}}\right]^2 \quad (3)$$

Table 3. Azeotropic data of the water-EDA system and boiling points of the pure components at different pressures

Pressure	(mmHg)	(bar)	Azeotropic composition (mol A)		Azeotropic temperature (K)		Boiling point (K), Water (A)	Boiling point (K), EDA (B)
			Built-in	Optimized	Built-in	Optimized		
Low pressure	100.0	0.133	0.4778	0.4804	342.36	343.07	324.71	337.11
	200.0	0.267	0.4592	0.4593	358.12	358.28	339.58	353.18
	400.0	0.533	0.4292	0.4284	375.82	375.36	356.10	371.41
	600.0	0.800	0.4094	0.4088	387.22	386.31	366.65	383.22
Atmospheric pressure	760.0	1.01325	0.3876	0.3558	394.27	393.07	373.14	390.54
High pressure	1345.2	1.793	0.3469	0.2345	412.67	410.26	389.97	409.65
	2044.4	2.726	0.3171	-	427.53	-	403.45	425.09
	2774.0	3.698	0.2861	-	439.19	-	413.97	437.18
	3480.8	4.641	0.2544	-	448.35	-	422.21	446.66
	4195.2	5.593	0.2455	-	456.22	-	429.27	454.78
	4909.6	6.546	0.2247	-	463.10	-	435.43	461.87

Table 4. Deviations between the experimental and calculated data at different pressures and the optimized NRTL parameters

Expt. date set #	Constant pressure (mmHg)	Sum of squares		Optimized NRTL BIPs		
		Built-in BIPs	Optimized BIPs	B_{12}	B_{21}	α_{12}
1	100.0	0.86705	0.58966	1283.4	−637.27	0.64049
2	200.0	0.40360	0.38895	1201.0	−564.60	0.76840
3	400.0	0.36747	0.28574	1070.7	−497.64	0.94064
4	600.0	0.42515	0.14673	956.41	−453.00	1.1086
5	760.0	0.52617	0.12403	899.34	−427.00	1.2210
6	1345.2	0.49754	0.08513	147.90	−403.26	0.99862
7	2044.4	0.57350	0.01869	A_{12}=−51.005 B_{12}=21925	A_{21}=10.234 B_{21}=−4676.5	1.4140
8	2774.0	0.70172	0.02614	2196.5	−228.38	2.4834
9	3480.8	0.89992	0.00518	856.07	−171.61	5.0641
10	4195.2	0.93227	0.04018	215.32	−211.32	3.7026
11	4909.6	0.74664	0.04341	212.93	−206.72	3.8020

After regression, the deviation between the NRTL plot and experimental VLE data was minimized and the optimized NRTL BIPs were obtained. Table 4 summarizes the deviations between the experimental and calculated data at different pressures using the built-in and optimized NRTL BIPs. The built-in parameters in PRO/II were replaced with the optimized parameters. The optimized NRTL BIPs of water-EDA at different pressures are also summarized in Table 4. By applying the optimized parameters, the azeotropic composition and temperature were adjusted subsequently. The azeotropic data based on the optimized NRTL plot are tabulated in Table 3. As can be noticed from the table, the azeotropic data at high pressure are not available since the azeotrope breaks as it approaches high pressure.

The experimental VLE data at different pressures were plotted against the T-x-y diagrams based on NRTL model using the built-in and optimized parameters. The VLE diagrams are illustrated accordingly in Figs. 2(a)-(d) for low pressures, Fig. 3 for atmospheric pressure, and Figs. 4(a)-(f) for high pressures. At low and atmospheric pressure, the built-in and optimized NRTL plot show that water-EDA system forms an azeotropic curve and the azeotropic composition decreases as pressure increases. The difference between the built-in and optimized NRTL plot at low pressure was not so visible, unlike in the case of high pressure. Though the built-in plot at high pressure shows an azeotropic behavior, the optimized plot

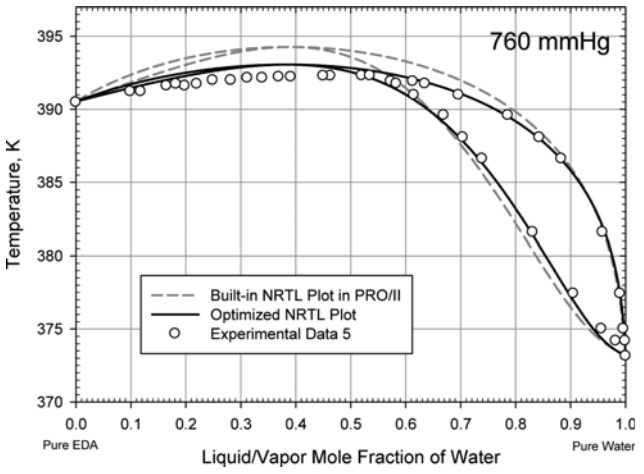

Fig. 3. T-x-y diagram of experimental VLE data against NRTL model using the built-in and optimized parameters at atmospheric pressure.

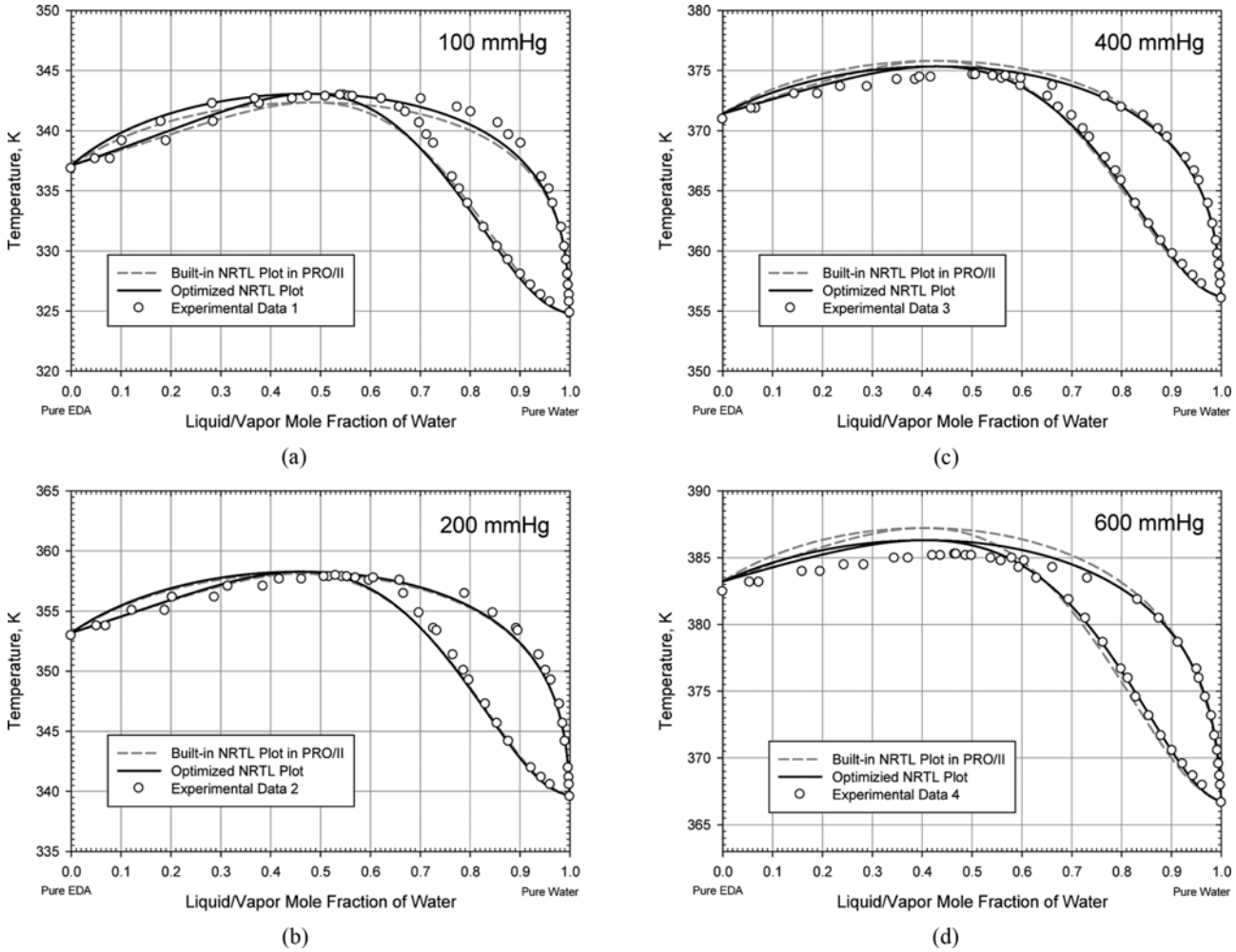

Fig. 2. T-x-y diagram of experimental VLE data against NRTL model using the built-in and optimized parameters at low pressure.

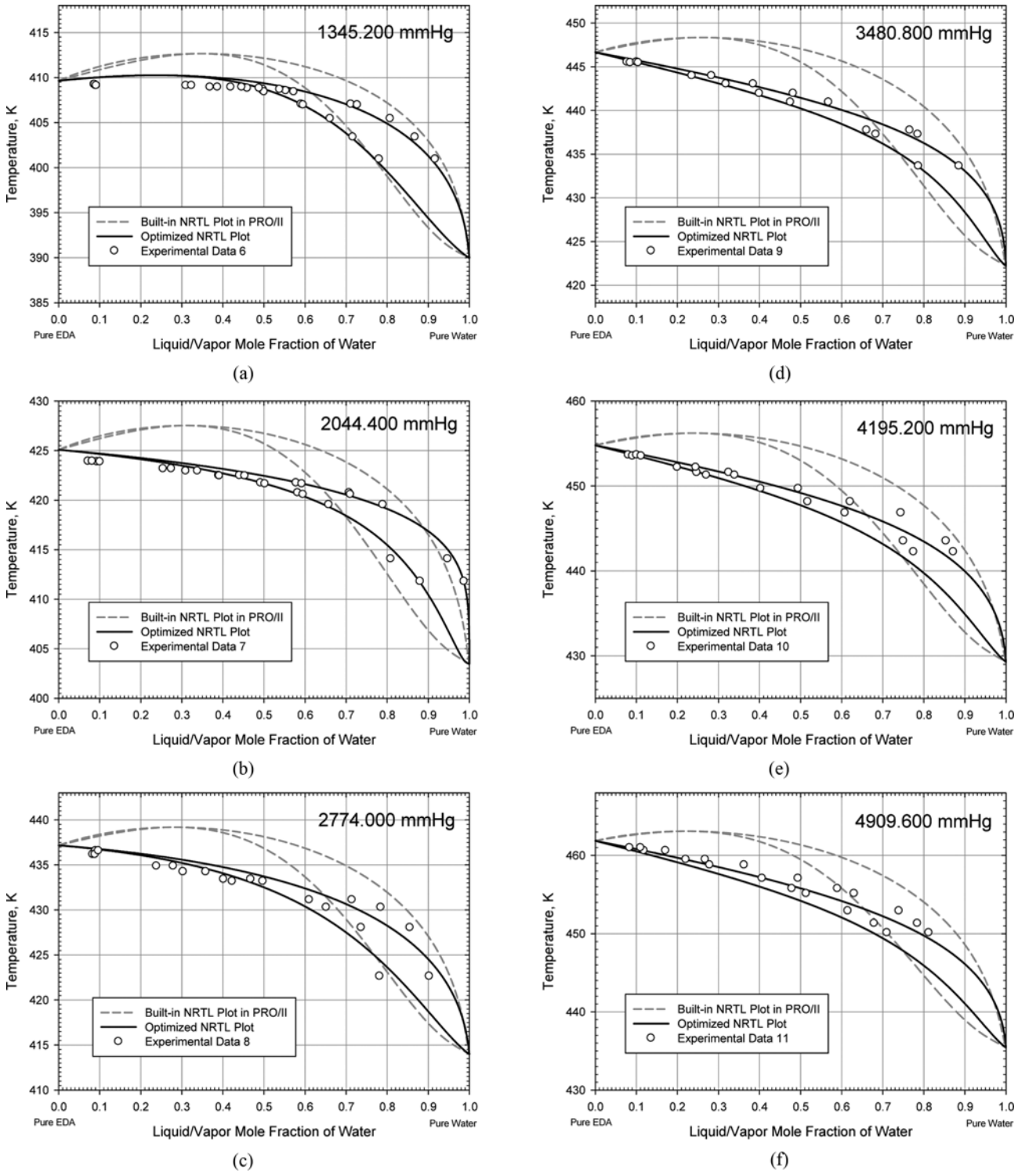

Fig. 4. T-x-y diagram of experimental VLE data against NRTL model using the built-in and optimized parameters at high pressure.

based on experimental VLE data differs greatly from the existing plot, and the azeotropic behavior of the water-EDA system breaks completely as the pressure increases.

As the pressure varied, the change in azeotropic composition was relatively small. Therefore, the operating pressures for the low-pressure (LP) and high-pressure (HP) column of PSD should be chosen appropriately in order to generate a feasible separation of water-EDA mixture.

PROCESS SIMULATION

The vapor-liquid equilibrium of water-EDA system was stud-

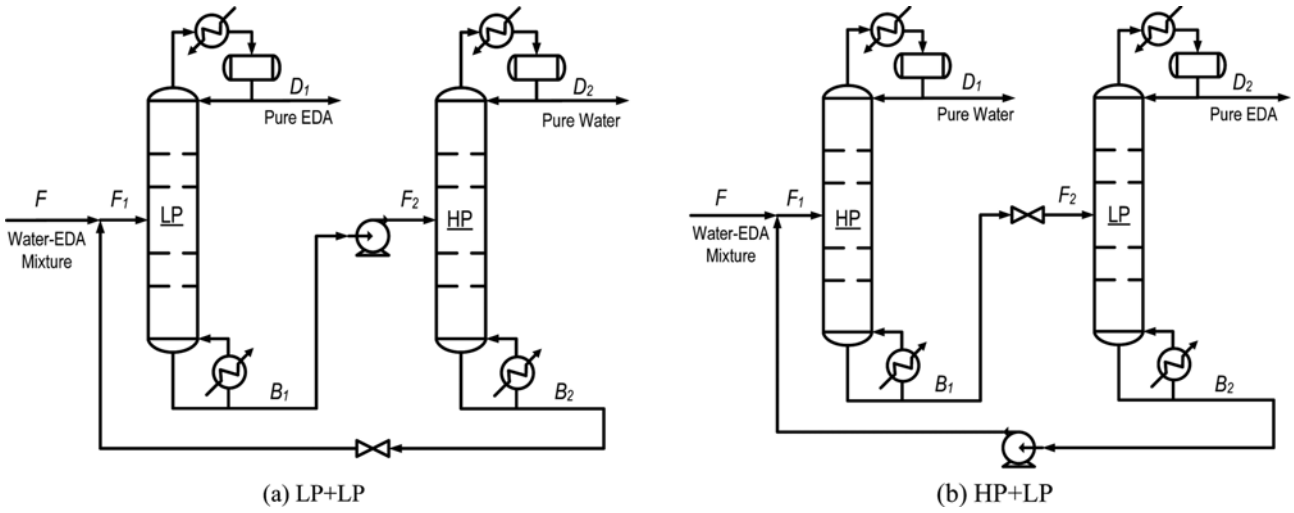

Fig. 5. PSD process flow diagram for water-EDA separation.

ied at different pressures to determine the operating pressures for the PSD process. For the simulation of PSD process, different sets of operating pressure were applied and the PSD performance was analyzed. The column configuration of PSD was also operated interchangeably wherein the positions of the LP and HP column are switched. The PSD flow diagram is illustrated in Figs. 5(a) and 5(b) using LP+HP and HP+LP column configuration, respectively. Since water-EDA mixture involves a maximum-boiling separation, the distillates are the product streams and the bottoms are the circulating streams for both columns. The recycle streams are liquids that are not required to be vaporized. Therefore, even if the two operating pressures result to a relatively small change in the azeotropic composition, PSD can still be feasible.

1. Steady-state Conditions

Research studies on the separation of water-EDA mixture also used process simulation. Based on a research by Modla and Lang [11] on the feasibility of PSD methods, some of the steady-state conditions of the feedstock were obtained and used in the simulation of this study. The design conditions for the simulation are summarized in Table 5(a) for the feedstock characterization, Table 5(b) for product and distillation column specification, and Table 5(c) for equipment specifications and operating conditions of each simulation case. Simulation runs were made with the distillate and bottoms composition held at specific values. Since the distillate is the desired product for both columns, its composition is specified to be of high purity at 99.5 mol% EDA and 99.5 mol% water for LP

Table 5. Steady-state condition for PSD simulation

(a) Feedstock conditions

Component	Composition (%mol)
Water	40
EDA	60
Total flow rate (kg-mol/hr)	340
Temperature (°C)	25
Pressure (bar)	1.01325

(b) Product and distillation column specifications

Rigorous distillation column		
Specification	LP column	HP column
Distillate composition	99.5 mol% EDA	99.5 mol% water
Distillate flowrate	~204 kgmol/hr	~136 kgmol/hr
Column dP	0.1 bar	0.1 bar
Condenser condition	at Bubble temp.	at Bubble temp.

(c) Equipment specifications and operating conditions of each simulation case

Case no.	Column operating P (mmHg)			Valve outlet P (bar)		Pump outlet P (bar)	Bottoms composition (mol% water)		
	LP		HP				LP		HP
	Case A	Case B		Case A	Case B		Case A	Case B	
1	100	200	760	0.2	0.4	1.5	0.47	0.44	0.36
2	100	200	1345.2	0.2	0.4	2	0.47	0.44	0.24
3	100	200	2044.4	0.2	0.4	3	0.47	0.44	0.1
4	100	200	2774	0.2	0.4	4	0.47	0.44	0.1
5	100	200	3480.8	0.2	0.4	5	0.47	0.44	0.1
6	100	200	4195.2	0.2	0.4	6	0.47	0.44	0.1
7	100	200	4909.6	0.2	0.4	7	0.47	0.44	0.1

and HP column, respectively. However, the bottoms composition is specified to be near its azeotropic composition. Thus, the bottoms composition varies depending on the operating pressure of the column. For each PSD simulation case, different sets of operating pressures were used for the LP column and HP column. The operating pressure of the LP column is 100 mmHg and 200 mmHg for case A and B, respectively. For HP column, seven operating pressures were applied individually from case 1 to case 7. The outlet pressures of valve and pump were operated at a pressure which is a bit higher than the operating pressure of LP and HP columns, respectively.

2. Simulation Procedure

To start the simulation, the thermodynamic model to be applied for the water-EDA system was selected. In this study, NRTL model with UNIFAC fill options were selected and its built-in BIPs in PRO/II were replaced with the optimized parameters calculated from the data regression. After overwriting the existing parameters, the PSD process was modeled by initially using a shortcut column followed by rigorous distillation column. After getting the optimum values of the column specifications (number of theoretical stages, reflux ratio and feed tray location) and simulating the optimum PSD, the column configurations were interchanged and heat integration was applied to the PSD model.

2-1. Shortcut Column Modeling

The first step in creating an overall distillation column design is identifying the number of stages required for a certain degree of separation. The number of theoretical stages (N) is inversely proportional to reflux ratio (R). As N increases, the initial capital investment increases but R decreases, which can reduce the operational

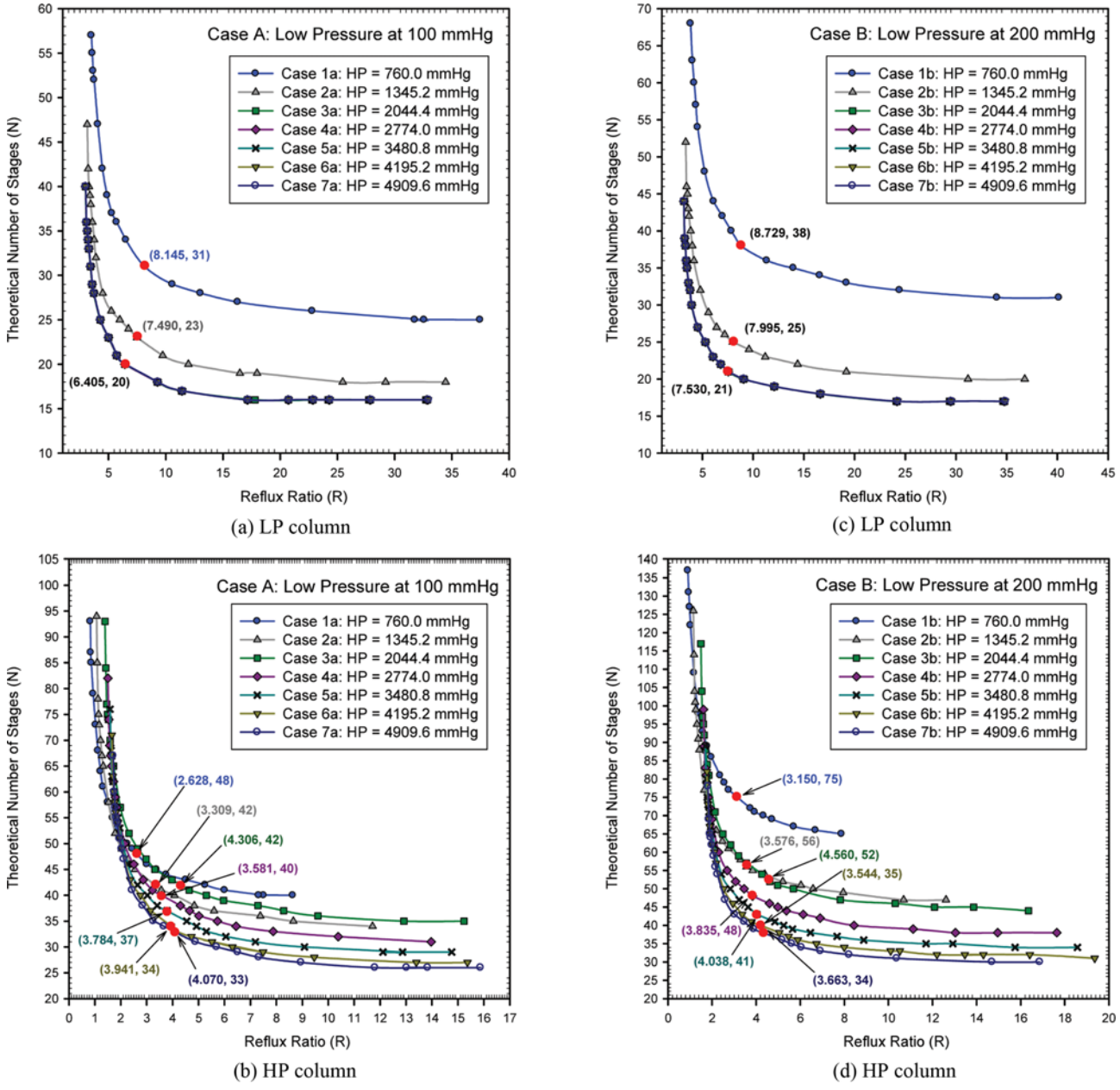

Fig. 6. Relationship of N and R with its optimum point.

Table 6. Minimum and optimum N and R based on shortcut column simulation result

Case no.	Operating pressure (mmHg)		N-min		R-min		N-opt		Total column stages	R-opt		Total column reflux ratios
	LP	HP	LP	HP	LP	HP	LP	HP		LP	HP	
1a		760.0	24	36	3.26	0.75	31	48	79	8.15	2.63	10.78
2a		1345.2	17	32	3.00	1.02	25	42	67	7.49	3.31	10.80
3a		2044.4	15	32	2.85	1.33	20	42	62	6.41	4.31	10.71
4a	100	2774.0	15	29	2.85	1.43	20	40	60	6.41	3.58	9.99
5a		3480.8	15	26	2.86	1.51	20	37	57	6.41	3.78	10.19
6a		4195.2	15	25	2.86	1.58	20	34	54	6.41	3.94	10.35
7a		4909.6	15	24	2.87	1.63	20	33	53	6.41	4.07	10.48
1b		760.0	29	58	3.49	0.79	38	75	113	8.73	3.15	11.88
2b		1345.2	19	43	3.20	1.10	25	56	81	8.00	3.58	11.57
3b		2044.4	16	41	3.01	1.42	21	52	73	7.53	4.56	12.09
4b	200	2774.0	16	35	3.02	1.53	21	48	69	7.53	3.84	11.37
5b		3480.8	16	31	3.02	1.62	21	41	62	7.53	4.04	11.57
6b		4195.2	16	29	3.03	1.68	21	35	56	7.53	3.54	11.07
7b		4909.6	16	27	3.03	1.73	21	34	55	7.53	3.66	11.19

cost. However, as R increases, the operational cost would be higher, but N will approach the minimum cost. The optimum values of N and R must be determined for a more economical separation process.

Using the shortcut column model in PRO/II, minimum reflux calculation was performed to determine the minimum values of N and R. For the column specification, the top and bottom compositions were specified. The graphs of N and R were generated from the results of shortcut column simulation, and the optimum values of N and R were identified based on the slope, which was inclined sharply from its tipping point.

2-2. Rigorous Column Modeling

After identifying the number of theoretical stages of each column, it was applied for the simulation of rigorous column. For the column specifications and variables, the distillate composition and distillate flow rate were set as parameters, while the heat duties of condenser and reboiler were set as variables. Selection of optimum feed tray locations is critical in maximizing distillation column performance. Using the case study option in PRO/II, the feed stage location for LP and HP column were varied to determine which among the combination of LP and HP feed stage could give the minimum total reboiler heat duty for each case. Since feed tray locations for each columns have not yet been determined, the initial assumptions of column feed stage were specified somewhere in the middle part of the column. The optimum feed tray locations were identified and applied for the complete simulation of the optimized PSD.

2-3. Column Configuration

Based on the results of shortcut and rigorous column modeling, the most economical process (with respect to the total number of theoretical stages, actual reflux ratio, and overall heat duty consumption) among the PSD cases can be determined. After identifying which among the cases give the lowest total N, total R, and overall heat duty consumption, that PSD case was further analyzed by interchanging its column configuration and checked whether it could give a better result. Since the previous simulation for each PSD case was operated at LP+HP column configuration, further simulation was changed to HP+LP column configuration wherein the first column operated at high pressure and the second column at low pressure.

2-4. Heat Integration

The energy consumption for a PSD process is quite high since the two distillation columns operate at two different pressures which yield to low temperature in one column and high temperature in the other column. Therefore, heat integration was applied to the PSD system to lessen the low- and high-temperature utility consumptions. For each case, either an auxiliary reboiler or condenser

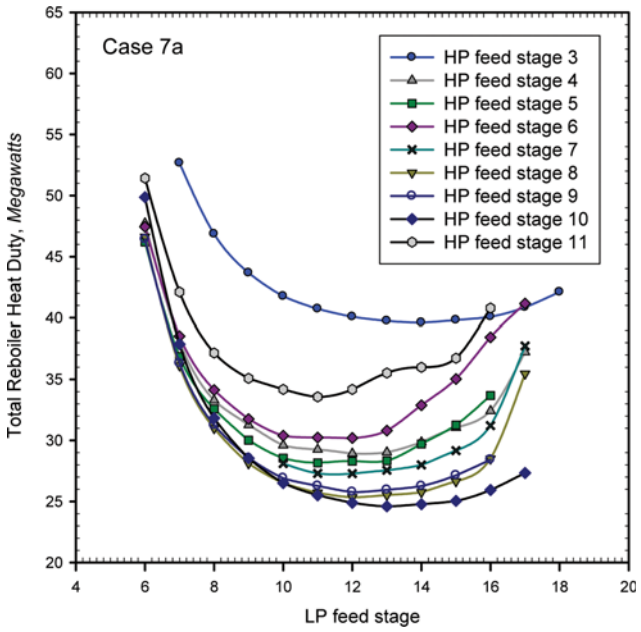

Fig. 7. Total reboiler heat duty with respect to LP feed stage based on various HP feed stage (case 7a).

could be required depending on the calculated heat duties from the simulation of a non-heat integrated PSD. If the heat duty of the LP reboiler is higher than the heat duty of the HP condenser, then an auxiliary reboiler is needed to provide the remaining heat required for the total heat input. In contrast, if the heat duty of the HP condenser is higher than that of the LP reboiler, an auxiliary condenser will be needed.

RESULTS AND DISCUSSION

The analysis and optimization of the separation method through PSD were performed using a process simulator. The simulation results for each PSD cases were summarized and discussed as follows.

1. Shortcut Column Simulation

Minimum reflux calculation was performed and the minimum values of N and R were determined for each PSD case. Based on the shortcut column simulation result, the graph of N versus R was created for LP and HP column separately and the optimum point was identified as shown in Figs. 6(a) and 6(b) for case A and Figs. 6(c) and 6(d) for case B. For LP column, the graph for cases 3-7 are the same; thus, the optimum values of N and R are also the same. As can be seen from the graph for HP column, the optimum N is decreasing while the optimum R is increasing from case 1 to case 7. The minimum and optimum values of N and R obtained for each PSD case are summarized in Table 6. The table also shows the total number of column stages and total column reflux ratios for each PSD case. The optimum N was used for the simulation of rigorous column, and the PSD process was further optimized by finding the optimum feed stage for each column.

2. Rigorous Column Simulation

Through case study of the rigorous column, the optimum feed tray location was identified based on the minimum total reboiler heat duty. Fig. 7 shows the graph of total reboiler heat duty with

Table 7. Optimum feed stage and minimum total heat duty based on rigorous column simulation results

Case no.	Feed stage		Actual reflux ratio		Heat duty (REBOILER), MW		Heat duty (CONDENSER), MW		Total heat duty	
	LP	HP	LP	HP	LP	HP	LP	HP	Reboiler	Condenser
1a	-	-	-	-	-	-	-	-	Too high	Too high
2a	-	-	-	-	-	-	-	-	Too high	Too high
3a	12	5	6.09	12.11	15.43	22.00	−17.28	−19.47	37.43	−36.74
4a	14	8	5.66	8.36	13.95	16.71	−16.25	−13.69	30.66	−29.94
5a	12	8	6.31	5.78	16.23	12.15	−17.82	−9.81	28.37	−27.63
6a	11	7	6.16	7.34	16.20	13.94	−17.45	−11.93	30.14	−29.38
7a	12	10	5.29	5.22	16.01	11.61	−15.34	−8.81	27.62	−24.15

Table 8. Comparison of results for column configurations and heat integration

Column configuration		LP+HP		HP+LP	
CASE		A	B	A	B
Operating pressure (mmHg)	LP	100	200	100	200
	HP	4909.6			
No heat integration					
Heat duty, megawatts (MW)	LP column condenser	−15.34	−18.19	−12.72	−12.48
	HP column condenser	−8.81	−10.42	−11.44	−13.30
	LP column reboiler	16.01	16.44	10.25	10.02
	HP column reboiler	11.61	13.11	14.68	16.70
Total heat duty, MW	Condenser	−24.15	−28.61	−24.15	−25.77
	Reboiler	27.62	29.55	24.94	26.72
Overall heat consumption, MW		**51.77**	**58.16**	**49.09**	**52.49**
Partial heat integration					
Heat duty, megawatts (MW)	LP column condenser	−15.34	−18.19	−12.72	−12.48
	Integrated heat exchanger	−8.81	−10.42	−11.44	−13.30
	Auxiliary reboiler/condenser	7.20	6.02	−1.18	−3.28
	HP column reboiler	11.61	13.11	14.68	16.70
Overall heat consumption, MW		**42.97**	**47.74**	**40.02**	**45.75**
Heat duty reduction		*17.01%*	*17.92%*	*18.48%*	*12.84%*

respect to LP feed stage based on various HP feed stage. The graph shows only the result for case 7a, but the same procedure was applied to the other cases. The summary of results for rigorous column modeling was tabulated on Table 7, which only shows the results for case A. There are no results shown for cases 1 and 2 since the simulation did not converge successfully and the total reboiler heat duty calculated was too high. Different combinations of optimum LP and HP feed stage were obtained for each case and the actual reflux ratios were calculated. Case 7a gives the lowest total heat duty of the reboiler and condenser.

3. Column Configuration and Heat Integration

Since case 7a has the lowest energy consumption according to the result of rigorous column modeling, further simulations were performed wherein the column configuration was changed from LP+HP to HP+LP. The simulation for case 7b was also analyzed as well as its column configuration change. The comparison of results for column configuration and heat integration is summarized in Table 8. Based on the results using the two column configurations, Case A gives a lower overall heat duty consumption compared to Case B. Between the two column configurations, HP+LP yields to

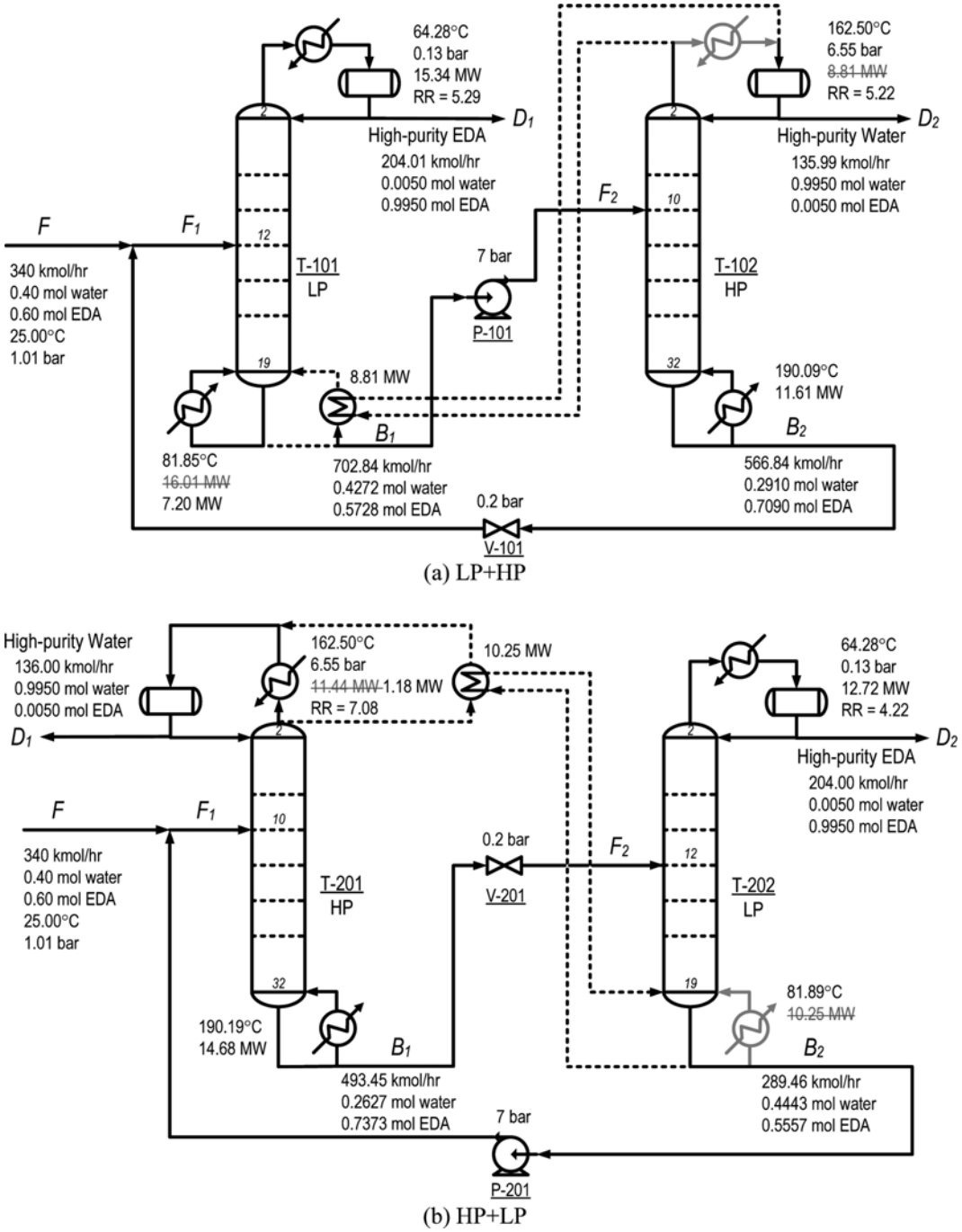

Fig. 8. Process flow diagram of optimum PSD design.

a lower energy consumption than the LP+HP column configuration. With the application of partial heat integration, the overall heat consumption can be reduced by 17.01% and 17.92% using LP+HP, and 18.48% and 12.84% using HP+LP for case A and case B, respectively.

4. Optimum PSD Process

As can be depicted from the comparison of results, case A gives the lowest overall heat consumption using both column configurations. To analyze the optimum PSD design systematically, a flow diagram of the overall process was drawn as illustrated in Figs. 8(a) and 8(b) using LP+HP and HP+LP column configurations showing the stream compositions and conditions, column specifications, and heat consumptions of the reboiler and condenser. The partial heat integration was also reflected in the process flow diagram with the corresponding conditions of integrated heat exchanger and auxiliary reboiler/condenser. As shown in the figure, an auxiliary reboiler was used for the LP+HP column configuration, while an auxiliary condenser was used for the HP+LP column configuration.

CONCLUSIONS

The separation of a maximum-boiling azeotropic mixture of water-EDA through PSD is possible even though the difference between the azeotropic composition using low and high pressure is relatively small. The deviation between experimental VLE data at different pressures and NRTL plot diminished after thermodynamic data regression was performed and the built-in parameters were replaced with the optimized parameters. From the shortcut column modeling, the number of theoretical stages was identified, and among the PSD cases, case 7a (LP: 100 mmHg & HP: 4,909.6 mmHg) has smallest total number of stages. Case 7a also gives the lowest total heat duty. When the LP and HP columns were interchanged, the HP+LP column configuration showed a lower overall heat duty compared to the LP+HP column configuration. After the application of heat integration, the overall heat consumption was reduced significantly.

ACKNOWLEDGEMENT

This research was supported by a grant from LNG Plant R&D Center founded by Ministry of Land, Transportation and Maritime affairs (MLTM) of the Korean government. This work was also supported by the Human Resources Development Program (No. 20134030200230) of the Korea Institute of Energy Technology Evaluation and Planning (KETEP) grant funded by the Korea government Ministry of Trade, Industry and Energy.

NOMENCLATURE

a_{ij}, b_{ij}, c_{ij}, d_{ij}, e_{ij}, f_{ij} : binary parameters in NRTL equation
A_{12}, A_{21}, B_{12}, B_{21} : binary interaction parameters
G_{ji}, G_{ki}, G_{kj} : binary parameter in NRTL equation
K : equilibrium constant [y/x ratio]
P : pressure [mmHg, bar]
T : temperature [°C, K]
w_i : objective function coeffiecient with respect to component i
x_j, x_k : mole fraction of component j and k in the liquid phase

Greek Symbols

α_{12} : non-randomness parameter
γ_i : activity coefficient of component i
τ_{ij}, τ_{ji}, τ_{kj} : binary parameter in NRTL equation

REFERENCES

1. The DOW Chemical Company©. DOW Specialty Amines. (1995-2015), http://www.dow.com/amines/prod/ethyl-eda.htm/.
2. J. Ledgard, *The Preparatory Manual of Explosives*, 3rd Ed., 59 (2007).
3. L. M. Mukherjee and S. Bruckenstein, Preparation of anhydrous ethylenediamine, *Pure Appl. Chem.*, 421 (2008).
4. M. Lichtenwalter, US Patent, 3,055,809A (1958).
5. W. Shen, H. Benyounes and V. Gerbaud, *Ind. Eng. Chem. Res.*, **52**(12), 4606 (2013).
6. W. Li, L. Shi, B. Yu, M. Xia, J. Luo, H. Shi and C. Xu, *Ind. Eng. Chem. Res.*, **52**(23), 7836 (2013).
7. E. K. Hilmen, *Separation of azeotropic mixtures: Tools for analysis and studies on batch distillation operation: A Thesis*, Norwegian University of Science and Technology, 30 (2000).
8. M. F. Doherty, Z. T. Fidkowski, M. F. Malone and R. Taylor, *Perry's Chemical Engineers' Handbook*, 8th Ed., 13-82 (1992).
9. W. L. Luyben, *Ind. Eng. Chem. Res.*, **47**(16), 6140 (2008).
10. W. L. Luyben, *Ind. Eng. Chem. Res.*, **51**(33), 10881 (2012).
11. G. Modla and P. Lang, *Chem. Eng. Sci.*, **63**(11), 2856 (2008).
12. G. Modla, *Comput. Chem. Eng.*, **34**(10), 1640 (2010).
13. G. Modla and P. Lang, *Dynamics and Control of Process Systems*, **2**, 361 (2007).
14. A. Kopasz, G. Modla and P. Lang, *Gépészet: Conference on Mechanical Engineering*, ISBN 978-963-420-947-8 (2008).
15. A. Kopasz, G. Modla and P. Lang, *Conference on Distillation Absorption*, Product composition control of a pressure swing double column batch rectifier, 557 (2010).
16. J. Fontalvo, M. A. G. Vorstman, J. G. Wijers and J. T. F. Keurentjes, *Design and performance of two-phase flow pervaporation and hybrid distillation processes: A Dissertation*, **7**, 111 (2005).
17. Finepac Structures Pvt. Ltd.© Ethylene diamine (EDA)-Water Separation System, http://www.finepacindia.in/applications.html/.
18. J. H. Lee, J. H. Cho, D. M. Kim and S. J. Park, *Korean J. Chem. Eng.*, **28**(2), 591 (2011).
19. Q. T. Sun, C. J. Pan and X. F. Yan, *Korean J. Chem. Eng.*, **30**(3), 518 (2013).
20. S. P. Shirsat, S. D. Dawande and S. S. Kakade, *Korean J. Chem. Eng.*, **30**(12), 2163 (2013).
21. J. M. Prausnitz, R. N. Lichtenthaler and E. G. de Azevedo, *Molecular thermodynamics of fluid-phase equilibria: A Book*, 3rd Ed., 258-291 (1998).
22. G. M. Kontogeorgis and G. K. Folas, *Thermodynamic models for industrial applications*, 109-154 (2010).
23. "PRO/II Reference Help", Invensys System Inc., SimSci-Esscor, 1994-2013. Revision: 25 Mar. 2013.